

# Theory of the optical properties of a DNA-modified gold nanoparticle system

Sung Yong Park\*, David Stroud

*Department of Physics, The Ohio State University, Columbus, Ohio, OH 43210, USA*

---

## Abstract

We describe a simple model for the melting and optical properties of a DNA/gold nanoparticle aggregate. The aggregate is modeled as a cluster of gold nanoparticles on a periodic lattice connected by DNA bonds, and the extinction coefficient is computed using the discrete dipole approximation. The optical properties at fixed wavelength change dramatically at the melting transition, which is found to be higher and narrower in temperature for larger particles, and much sharper than that of an isolated DNA link. All these features are in agreement with available experiments.

© 2003 Elsevier B.V. All rights reserved.

*PACS:* 61.43.Hv; 78.67.–n; 82.60.Qr; 87.15.–v

*Keywords:* Melting; Nanoparticle aggregate; DNA; Gold; Optical properties

---

## 1. Introduction

Recently, so-called functional metallic nanoparticles have started to be developed, which may lead to new materials with improved optical and mechanical properties [1]. Among these, there is a particular interest in gold nanoparticles to which noncomplementary oligonucleotides capped with thiol groups are attached (DNA-modified gold nanoparticle system), because in addition to a strategy using self-assembly of nanoparticles [2], biological detection is possible using the optical and electrical sensitivity of their aggregates [3,4].

In this paper, we present a model for this “melting” transition, which accounts for most experimentally observed features.

## 2. Structural modeling

To calculate the  $T$ -dependent optical properties, we have considered two slightly different structural models. In the simplest version of our model, the low- $T$  aggregate is taken simply as a collection of identical gold nanospheres (each of radius  $a$ ) which form a cube of edge  $L$  and fill the sites of a simple cubic lattice of lattice constant  $d$  ( $d > 2a$ ), containing  $N_{\text{par}} = (L/d)^3$  gold nanoparticles. We have also investigated the melting and the optical properties assuming that the low- $T$  cluster is a fractal aggregate. In both cases, we assume that all

---

\*Corresponding author. Tel.: +1-614-292-3298; fax +1-614-292-7557.

*E-mail addresses:* [parksy@mps.ohio-state.edu](mailto:parksy@mps.ohio-state.edu) (S.Y. Park), [stroud@mps.ohio-state.edu](mailto:stroud@mps.ohio-state.edu) (D. Stroud).

bonds are occupied by the same number ( $N_s/z$ ) of DNA links at low temperature, where  $N_s$  is the number of single DNA strands attached to one particle and  $z$  is the number of nearest neighbors ( $z = 6$  for a simple cubic lattice).

As temperature is increased, the bonds start to break. We define the probability that a link forms between a given gold particle pair at temperature  $T$  as  $p_{\text{eff}}(T)$ . To generate a specific sample at temperature  $T$ , we randomly remove links with probability  $1 - p_{\text{eff}}(T)$ , then identify the separate clusters, using a simple computer algorithm [5]. If the aggregate is separated into two or more clusters, we simply place these clusters in random positions and orientations within a larger bounding box (usually of edge  $100d$ ), taking care that the individual clusters do not overlap. The resulting geometry is shown schematically in Fig. 1. As a second structural model, we have carried out the same procedure to simulate the melting of a sample formed by reaction-limited cluster–cluster aggregation (RLCA). (For the actual computer algorithm to produce the RLCA clusters, see, e.g., Ref. [6].) A typical RLCA cluster is shown in Fig. 1(d), and represents a possible fractal aggregate which might be produced by certain random growth processes at low temperature [7]. Here, we implicitly assume that the specific bonds which are occupied at temperature  $T$  are time independent.

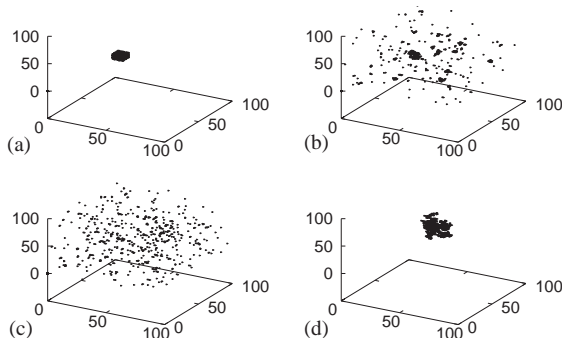


Fig. 1. Schematic of the melting of a gold–DNA cluster, for two different models discussed in the present paper. In the first model, (a) shows the cluster at low  $T$  ( $p_{\text{eff}} = 1$ ); (b)  $p_{\text{eff}} = 0.5 > p_c(L)$ , where  $p_c$  is the weakly  $L$ -dependent percolation threshold; (c)  $p_{\text{eff}}(T) = 0.2 < p_c(L)$ ; (d) alternate model for low- $T$  sample ( $p_{\text{eff}}(T) = 1$ ): fractal cluster formed by reaction-limited cluster–cluster aggregation [RLCA], with fractal dimension  $d_f \sim 2.1$ .

### 3. Melting theory for DNA links

The two-state model can describe melting well for short DNA strands (12–14 base pairs) [8,9], and is given by the relation

$$S + S \rightleftharpoons D. \quad (1)$$

The chemical equilibrium condition corresponding to Eq. (1) is

$$\frac{[1 - p(T)]^2}{p(T)} = \frac{K(T)}{C_T}, \quad (2)$$

where  $p(T)$  is a (temperature dependent) fraction of the double DNA strands,  $K(T)$  is a suitable chemical equilibrium constant, and  $C_T$  is the molar concentration of single DNA strands in the sample. We have also assumed the simple van't Hoff behavior  $K(T) = \exp[-\Delta G/k_B T]$ , with a Gibbs free energy of formation  $\Delta G(T) = c_1(T - T_M) + c_2(T - T_M)^3$ , choosing the values of  $c_1$ ,  $c_2$ , and  $T_M$  to be consistent with experiments on these DNA molecules.

In order to calculate the fraction  $p_{\text{eff}}(T)$  of bonds which contain at least one double strand, we adopt the following very simplified model. First, we assume that exactly  $N_s/z$  of the single strands on a given nanoparticle are available to bond with any one of its  $z$  nearest neighbors. Thus, we assume that the maximum number of links that could be formed between any two particles is  $N_s/z$ . The probability that *no* link is formed is then taken to be

$$1 - p_{\text{eff}}(T) = [1 - p(T)]^{N_s/z}. \quad (3)$$

In Fig. 2, we plot  $p_{\text{eff}}(T)$  for several radius  $a$ . We assume  $N_s \propto a^2$ , set  $z = 6$  and use the experimental result that  $N_s = 160$  when  $a = 8$  nm [10].

In actuality, there is a linker molecule which emerges from solution to connect two DNA single strands on different nanoparticles. But in fact, we can avoid considering the linker molecule explicitly, as shown in the inset of Fig. 2. In this inset, the dotted and dashed lines represent  $p(T)$  for two melting curves, one for each single strand connected to a linker molecule with slightly different constants  $c_1$  and  $c_2$  but the same melting temperature. (This is the case where the linker molecule is expected to have the most effect.) The solid line is

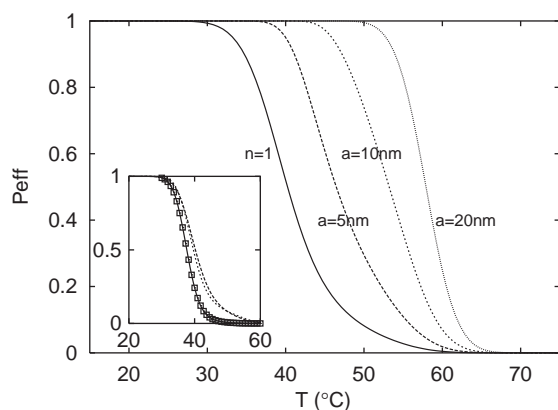


Fig. 2. Plot of  $p_{\text{eff}}(T)$  versus  $T$  for several different choices of particle radius  $a$ , as indicated. Also plotted is  $p(T)$ , the probability that a given DNA strand is part of a double strand at  $T$  (indicated as  $n = 1$ ). Inset: Comparison of  $p(T)$  and  $p'(T)$ .

the resulting melting curve for the two single strands plus linker. The squares are the melting probability  $p'(T)$  calculated assuming two effective strands and no linker strand with slightly different  $c_1$ ,  $c_2$ , and  $T_M$ .

#### 4. Optical properties

We calculate the optical properties of this sample using the discrete dipole approximation (DDA) [11,12]. The sample is modeled as a collection of separate aggregates, whose extinction coefficients are computed individually, then added. Each aggregate consists of many identical nanoparticles, which have complex frequency-dependent dielectric constant  $\varepsilon(\omega)$ , and polarizability  $\alpha(\omega)$  related to  $\varepsilon(\omega)$  by the Clausius–Mossotti equation with radiative reaction correction term [13]. The resulting expressions for the induced dipole moment  $\mathbf{p}_i$  of the  $i$ th sphere, and the corresponding expression for the extinction coefficient  $C_{\text{ext}}(k)$  at wave number  $k$ , are given in Ref. [14].

In our case, each cluster consists of a number of DNA-linked individual gold nanoparticles. In our calculations, we do not include the optical properties of the DNA molecules, since these absorb primarily in the ultraviolet [15]. We use tabulated values of the gold complex index of refraction

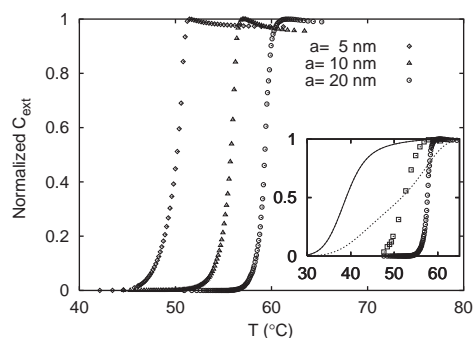


Fig. 3. Normalized extinction coefficient  $C_{\text{ext}}(\lambda, T)$  for  $\lambda = 520$  nm, plotted versus  $T$  for several particle radii  $a$ , assuming that the low- $T$  aggregate is an  $N = 1000$  simple cubic cluster, as shown in Fig. 1. Inset: Normalized extinction coefficient  $C_{\text{ext}}(\lambda, T)$ , versus  $T$  for  $\lambda = 520$  nm, plotted for a 1000-particle gold/DNA aggregate assuming that the low-temperature sample is a simple cubic cluster (open circles) or an RLCA cluster (open squares). The solid curve is a plot of  $1 - p(T)$  for a single DNA duplex with the same concentration  $C_T$  as the above two curves. The dotted curve represents  $1 - p(T)$  for a single DNA duplex but with a much higher  $C_T$  than for the other curves of the inset.

[16,17], then calculate  $C_{\text{ext}}$  for each cluster using the DDA. To improve the statistics, we average  $C_{\text{ext}}$  for each cluster over possible orientations. We then sum the averaged extinction coefficients of all the individual clusters to get the total extinction coefficient of the suspension. This method is justified when the suspension is dilute.

In Fig. 3, we show  $C_{\text{ext}}(\lambda, T)$  at fixed  $\lambda = 520$  nm, close to the isolated particle surface-plasmon resonance (SPR), versus  $T$ , for several particle sizes, assuming that the low- $T$  aggregate is a simple cubic cluster with  $N = 1000$  particles, which is illustrated in Fig. 1(a). As can be seen in Fig. 3, for each radius  $a$ , the extinction increases sharply at a characteristic temperature, corresponding to the melting of the aggregate for that size; at this temperature, the absorption due to the SPR increases sharply.

In the inset of Fig. 3, we compare  $C_{\text{ext}}(\lambda, T)$  for a regular and an RLCA cluster of particles of 20 nm radius at  $\lambda = 520$  nm, both for  $N = 1000$  particles. Although the RLCA cluster has a slightly broader melting transition, as manifested in  $C_{\text{ext}}(\lambda, T)$ , than does the regular lattice, both sets of data show a much sharper melting transition than that of a

single DNA link. Also, although our normalized  $C_{\text{ext}}(\lambda, T)$  is calculated for the aggregates at 520 nm, we expect similar behavior at 260 nm. (We have not carried out calculations at this  $\lambda$  mainly because we have not included the DNA absorption properties.) In any case, the experimental melting curves at 260 and 520 nm are very similar [18].

## 5. Discussion

We have briefly described a model for structural development of DNA/gold nanoparticle clusters, and have calculated the resulting cluster optical properties using the DDA.

Our calculated extinction coefficients are in good agreement with recent experimental results [3,15,18]. In particular, both experiment and calculation give a sharp increase in  $C_{\text{ext}}(\lambda, T)$  at fixed  $\lambda$ , as  $T$  increases past a critical temperature. We also find, in agreement with experiment, that melting occurs over a much narrower range of  $T$  in the aggregate than for a single bond, and that the melting occurs at higher  $T$  for larger particles.

## Acknowledgements

This work has been supported by NSF Grant DMR01-04987, by the U.S./Israel Binational Science Foundation, and by an Ohio State University Postdoctoral Fellowship. Calculations were carried out using the facilities of the Ohio Supercomputer Center.

## References

- [1] C. Sanchez, G.J. de A.A. Soler-Illia, F. Ribot, T. Lalot, C.R. Mayer, V. Cabuil, *Chem. Mater.* 13 (2001) 3061.
- [2] C.A. Mirkin, R.L. Letsinger, R.C. Mucic, J.J. Storhoff, *Nature* 382 (1996) 607.
- [3] R. Elghanian, J.J. Storhoff, R.C. Mucic, R.L. Letsinger, C.A. Mirkin, *Science* 277 (1997) 1078; J.J. Storhoff, R. Elghanian, R.C. Mucic, C.A. Mirkin, R.L. Letsinger, *J. Am. Chem. Soc.* 120 (1998) 1959.
- [4] S.-J. Park, T.A. Taton, C.A. Mirkin, *Science* 295 (2002) 1503.
- [5] D. Stauffer, A. Aharony, *Introduction to Percolation Theory*, 2nd Edition, Taylor and Francis, London, 1994.
- [6] W.D. Brown, R.C. Ball, *J. Phys. A* 18 (1985) L517; P. Meakin, *Adv. Colloid Interf. Sci.* 28 (1988) 249.
- [7] S.Y. Park, D. Stroud, *Phys. Rev. B* 67 (2003) 212 202.
- [8] V.A. Bloomfield, D.M. Crothers, I. Tinoco, Jr., *Nucleic Acids*, University Science Books, Sausalito, California, 2000.
- [9] H. Werntges, G. Steger, D. Riesner, H.-J. Fritz, *Nucleic Acids Res.* 14 (1986) 3773.
- [10] L.M. Demers, C.A. Mirkin, R.C. Mucic, R.A. Reynolds III, R.L. Letsinger, R. Elghanian, G. Viswanadham, *Anal. Chem.* 72 (2000) 5535.
- [11] E.M. Purcell, C.R. Pennypacker, *Astrophys. J.* 186 (1973) 705.
- [12] B.T. Draine, P.J. Flatau, *J. Opt. Soc. Am. A* 11 (1994) 1491.
- [13] B.T. Draine, *Astrophys. J.* 333 (1988) 848.
- [14] A.A. Lazarides, G.C. Schatz, *J. Phys. Chem. B* 104 (2000) 460 and references therein.
- [15] J.J. Storhoff, A.A. Lazarides, R.C. Mucic, C.A. Mirkin, R.L. Letsinger, G.C. Schatz, *J. Am. Chem. Soc.* 122 (2000) 4640.
- [16] D.W. Lynch, W.R. Hunter, in: E.D. Palik (Ed.), *Handbook of Optical Constants of Solids*, Academic, New York, 1985, p. 294.
- [17] P.B. Johnson, R.W. Christy, *Phys. Rev. B* 6 (1972) 4370.
- [18] C.-H. Kiang, *Physica A* 321 (2003) 164.